

Supporting information for:

Structure-dependent CO₂ reduction on molybdenite (MoS₂)
electrocatalysts

*Jake Limb, Lachlan F. Gaudin, Cameron L. Bentley **

School of Chemistry, Monash University, Clayton, Victoria 3800, Australia

E-mail: cameron.bentley@monash.edu

Contents

Section S1: Methods	3
Section S2: Pixel Selection	6
Section S3: Surface topography	7
Section S4: Basal plane activity	7
Section S5: Wetting/de-wetting on the crevice-like structure	8

Section S1: Methods

Probe fabrication

To prepare the nanopipette probes, borosilicate capillary tubes were used (BF100-50-10, Sutter Instruments, USA; dimensions: outer diameter, 1.0 mm; inner diameter, 0.5 mm; length 100 mm). The capillaries were placed in a capillary gravity-puller (PC-100, NARISHIGE Group, Japan) and pulled to ~230 nm tip diameter with the following parameters: Step (1) – One-step, NO. 1 (2) – 61.1, NO. 3 (3) – N/A, Weight (4) – 250g, Slider (5) – N/A. Probe diameter was verified by performing scanning electron microscopy (SEM) on a Quanta 3D FIB-SEM.

Electrode preparation

Bulk molybdenite (MoS_2) electrodes were prepared by using Scotch tape (Magic Invisible Tape, 810D) to pull off a small multilayer section of MoS_2 of ~4 mm² in size. This was then placed on a glass slide before conductive single-sided copper tape (AGG3940, Agar Scientific, UK) is placed over the top with a circular cut-out to expose the MoS_2 crystal. The edges of the copper tape were pressed down to ensure a solid electrical connection on the edges of the MoS_2 crystal. This electrode is then attached to an SEM stub (SEM pin stubs, Microscopy Solutions Pty. Ltd., Australia) using conductive double-sided copper tape (AGG3397, Agar Scientific, UK).

Electrolyte preparation

BMIM- BF_4 (io-li-tec, 99%) solution was prepared by mixing 10.6mol% IL (approx. 50:50 vol%, as previously reported due to the high current densities produced with ~90% water mole fraction)¹ in ultrapure water (resistivity 18.2 M Ω ·cm @ 25 °C, Direct-Q Water Purification System, Milli-Q, USA). BMIM- BF_4 solution was then transferred into the probes via capillary syringes (Microfil 34 gauge, 67mm long, World Precision Instruments).

QRCE Preparation and calibration

Quasi-reference counter electrodes (QRCEs) used in the probe are prepared through electrochemical oxidation of an Ag wire (Goodfellow, UK: thickness, 0.125mm; purity, 99.99%) in a saturated solution of KCl to form a

consistent anodized layer. To calibrate, the open circuit potential of the QRCE was measured against a leakless Ag/AgCl electrode in BMIM-BF₄ (10.6mol% in water) solution over a period of three hours. The QRCE potential is then compared against the more well-defined saturated calomel electrode (SCE) (CHI150, CH Instruments, Inc., USA). The QRCE was found to possess a stable value of 0.116 V vs. SCE.

Scanning Electrochemical Cell Microscopy (SECCM) Measurements

SECCM measurements on these samples are done through a custom-built scanning electrochemical probe microscope set up as previously reported,² consisting of a piezoelectric positioner (200 μm × 200 μm × 200 μm range, Nano-3D200, MadCityLabs, USA) to position the probes above the working electrode surface. During operation, the probe tip is inserted through a small hole (~4mm diameter) in the lid of a polypropylene plastic container (HPL931, 100mL, Lock&Lock, South Korea) which holds the substrate to control the environment (i.e., atmosphere and humidity levels), as previously reported.³ A gas inlet port (Omnifit Connector, Kinesis, UK) enabled the supply of N₂ and CO₂ into the cell which passes through a gas sparger filled with saturated NaCl solution and controlled through a variable area flow meter (2510 2A12, Brooks Instrument, USA) to maintain a constant supply of ~100cm³ min⁻¹, where it travels through a small inlet on the side of the container. Two holes placed in the lid were replaced by cover glass (thickness: 0.13 – 0.17 mm, dimensions: 24×50mm²) to supply the sample with light and an optical pathway to view the probe tip at the surface using an optical camera (Axiocam ERc5s, ZEISS, Germany) fitted with a magnification lens (44mm/3.00× InfiniStix, Infinity USA). This entire set up was placed on an optical breadboard to which the positioner, environmental cell and camera were mounted, and this breadboard was attached to a vibration isolation stage (25BM-8, Minus K Technology, USA). The vibration isolation stage with the above attachments were placed in a home-built aluminium Faraday cage to suppress electrical noise from other instruments. To make an electrical connection through the system, the Ag/AgCl QRCE is placed in the electrolyte-filled nanopipette probe, and the prepared MoS₂ surface was connected to a variable-gain low-noise current amplifier (DLPCA-200, FEMTO, Germany).

The SECCM experiment was conducted in hopping-mode with the tip being repeatedly approached to the surface and moved horizontally back and forth to produce maps of variable size (e.g., 40 × 50 μm²) grids of measurements that were used to obtain spatially resolved electrochemical information in the form of LSVs. At each location the tip was approached toward the surface with an applied potential ($E_{app} = 0.88$ V) on the QRCE

(held at 0 V with respect to the ground). This was until the electrolyte meniscus protruding from the tip contacted the surface, inducing a double-layer charging current. When this charging current exceeded 3.5 pA, the approach was stopped, and the potential was stepped to $E = -0.08$ vs. SCE and a potential range is swept up to -1.28 V vs. SCE at a scan rate of 1 V s^{-1} . Finally, the tip was moved away from the surface before being positioned on the next scan location, with the above process being repeated until a full grid of measurements were obtained. A scan is conducted under N_2 environment then the MoS_2 sample is subsequently washed in ultrapure water to remove debris left by the electrolyte and then conducted under CO_2 . It should be noted that since the potential was applied at the QRCE, not the surface, the surface potential (E_{surf}) is opposite to that of the QRCE ($E_{\text{surf}} = -E_{\text{app}}$). Positioning of the probe is monitored, and the z-piezo position at each scan location was used to generate topographical maps of the scan area. The data acquisition was handled by an FPGA card (NI USB-7855R, National Instruments, USA), which sat between the LabVIEW interface (running the Warwick Electrochemical-Scanning Probe Microscopy Platform [WEC-SPM], <https://warwick.ac.uk/fac/sci/chemistry/research/electrochemistry/>) and the SECCM instrument.

Imaging

Optical imaging was completed on a reflection mode optical microscopy system (Axiolab 5, ZEISS, Germany) fitted with an Axiocam 105 colour and processed using ZEN imaging software (publicly available from: zeiss.com/microscopy/en/products/software/zeiss-zen.html). Post-scan co-location and imaging was completed on an SEM (FEI Quanta FEGSEM) which enabled measurement of the surface areas of the droplet contact to the surface. Measurement of probe tip diameters is completed via coating the probes with iridium to act as a conductive layer.

Data processing

All data acquired in these experiments is processed through the MATLAB R2020a (MathWorks, USA) software package and subsequently plotted using both MATLAB R2020 and the python Matplotlib package. Electrochemical activity maps are uninterpolated and are produced by taking the surface current at $E = -1.28$ V at each point. Topography map shown in Figure S2 is processed using Gwyddion (<http://gwyddion.net/>). All histogram plots shown are binned with a consistent $0.1 \log_{10}|i(\text{pA})|$ due to the small amount of data points present in each plot as opposed to using a more standardised route such as making use of the Freedman-

Diaconis rule to determine the binning value.⁴ Figure S4b contains a binning value of 0.35 due to the low variability in currents present on the relatively inactive BP. Each histogram is accompanied by a KDE line which depicts an estimate of the probability density function for the histogram, aiding in recognising different modality patterns that some of these features present with. The Bandwidth of this KDE is determined by Scott's Rule.⁵

Section S2: Pixel Selection

Pixels chosen to represent combined LSVs of each representative structure. note that the pixels chosen in Figure S1d are where the step edge structure should appear but does not due to the lack of activity.

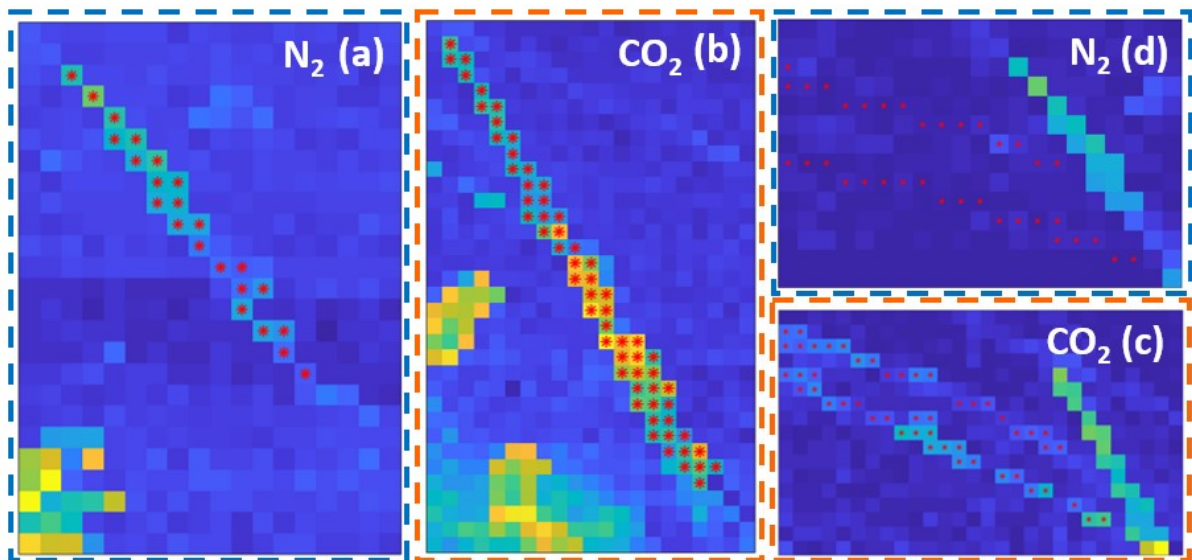


Figure S1. Pixel selection for representative LSVs for the main feature (Figure 1b,c) in **(a)** N₂ atmosphere and **(b)** CO₂ atmosphere, and pixel selection for the step edge feature (Figure 3a,b) in **(c)** CO₂ atmosphere and **(d)** N₂ atmosphere.

Section S3: Surface topography

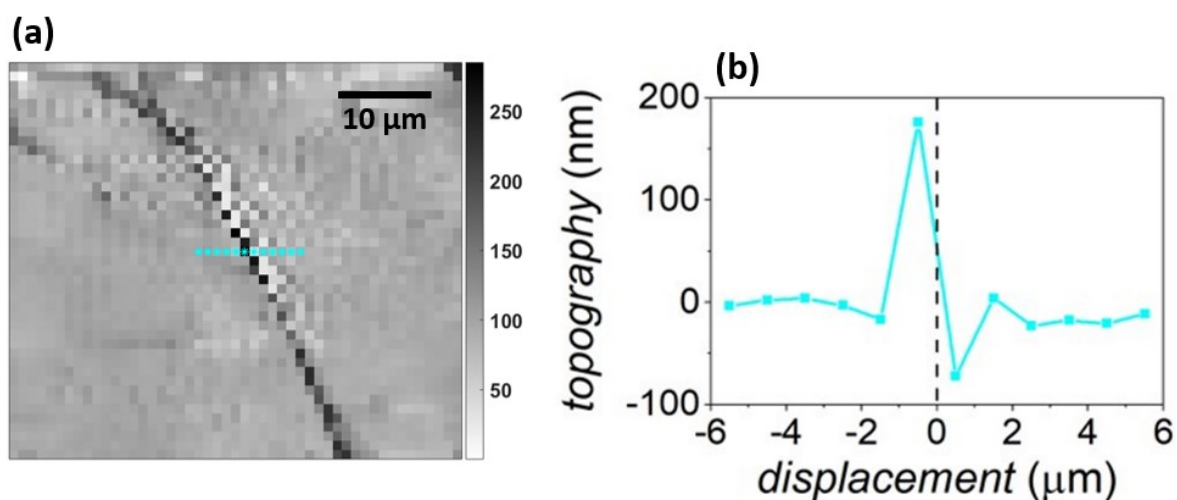


Figure S2. (a) Topographical map of entire scan area, constructed from the piezo positions recorded during the SECCM scan taken under a CO₂ atmosphere with the corresponding (b) displacement line, depicting a >200 nm height increase over the main structure.

Section S4: Basal plane activity

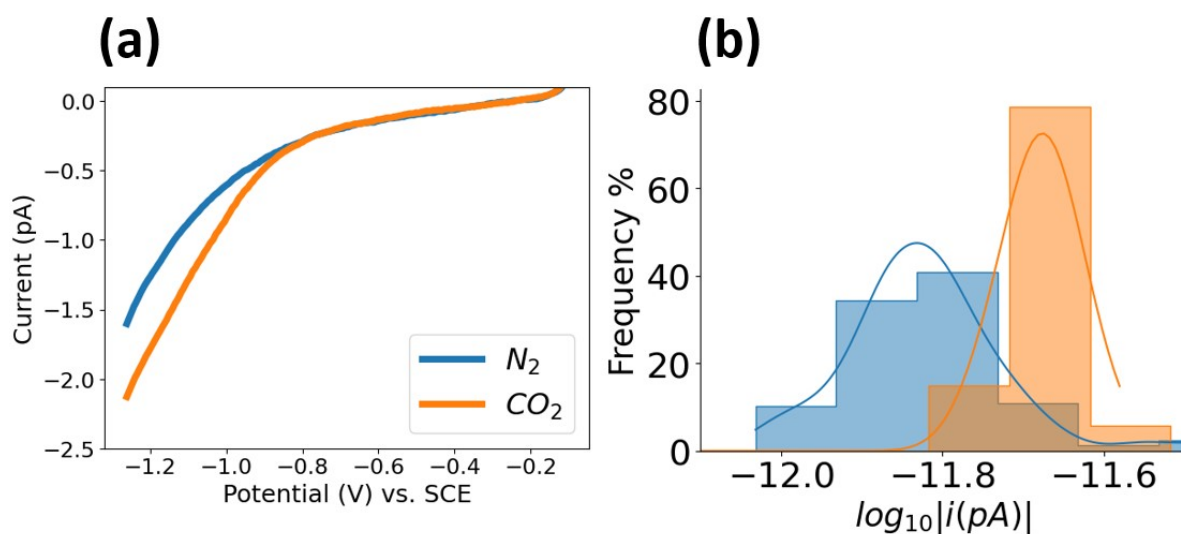


Figure S3. (a) Median LSVs of the basal plane in both N₂ and CO₂ atmospheres with corresponding (b) histogram N₂ atmosphere and CO₂ atmosphere at $E = -1.28$ V vs. SCE, 1 V s^{-1} scan rate with a binning value of $0.35 \log_{10}|i(\text{pA})|$.

Section S5: Wetting/de-wetting on the crevice-like structure

A few select LSVs are depicted below in Figure S4a which show the aberrations in the measured currents produced from the rapid 'wetting' and 'de-wetting' process that is proposed, all LSVs eventually converge to the same activity at $E = -1.28$ V vs. SCE.

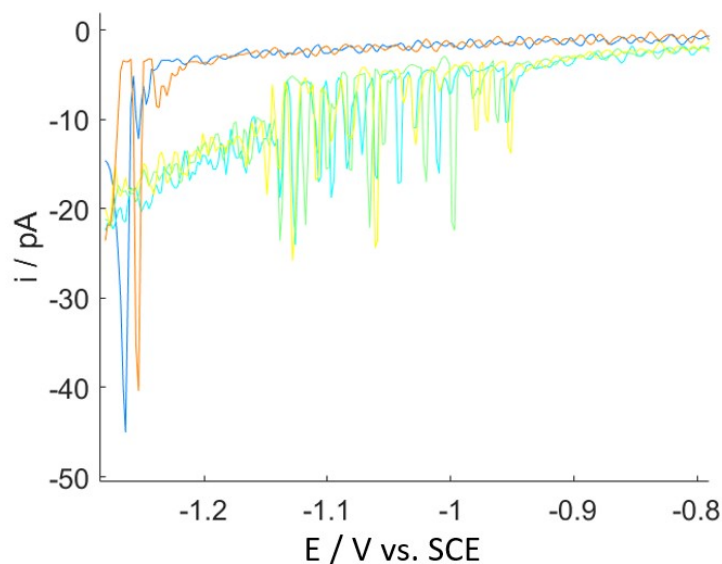


Figure S4. **(a)** Five example LSVs taken from Figure S1b which show large spikes in the measured current caused by sporadic wetting/de-wetting into the crevice structure.

References

- (1) Asadi, M.; Kumar, B.; Behranginia, A.; Rosen, B. A.; Baskin, A.; Repnin, N.; Pisasale, D.; Phillips, P.; Zhu, W.; Haasch, R.; et al. Robust carbon dioxide reduction on molybdenum disulphide edges. *Nat Commun* **2014**, *5*, 4470. DOI: 10.1038/ncomms5470.
- (2) Bentley, C. L.; Gaudin, L. F.; Kang, M. Direct electrochemical identification of rare microscopic catalytic active sites. *Chemical Communications* **2023**, *59* (16), 2287-2290, 10.1039/D2CC06316F. DOI: 10.1039/D2CC06316F.
- (3) Ornelas, I. M.; Unwin, P. R.; Bentley, C. L. High-Throughput Correlative Electrochemistry–Microscopy at a Transmission Electron Microscopy Grid Electrode. *Analytical Chemistry* **2019**, *91* (23), 14854-14859. DOI: 10.1021/acs.analchem.9b04028.
- (4) Freedman, D. A.; Diaconis, P. On the histogram as a density estimator:L2 theory. *Zeitschrift für Wahrscheinlichkeitstheorie und Verwandte Gebiete* **1981**, *57*, 453-476.
- (5) Scott, D. W. *Multivariate Density Estimation: Theory, Practice, and Visualization*; Wiley, 2015. DOI: 10.1002/9781118575574.